Deeply Virtual Compton Scattering with CLAS12 at Jefferson Lab

Adam Hobart[1,*] for the CLAS collaboration

[1]Université Paris-Saclay, CNRS/IN2P3, IJCLab, 91405 Orsay, France

Abstract. A key step toward a better understanding of the nucleon structure is the study of Generalized Parton Distributions (GPDs). GPDs are the object of an intense effort of research since they convey an image of the nucleon structure where the longitudinal momentum and the transverse spatial position of the partons inside the nucleon are correlated. Moreover, GPDs give access, via Ji's sum rule, to the contribution of the orbital angular momentum of the quarks to the nucleon spin, which is important to the understanding of the origins of the nucleon spin. Deeply Virtual Compton scattering (DVCS), the electroproduction of a real photon off the nucleon at the quark level, is the golden process directly interpretable in terms of GPDs of the nucleon. The GPDs are accessed in DVCS mainly through the measurements of single- or double- spin asymmetries. Combining measurements of asymmetries from DVCS experiments on both the neutron and the proton will allow us to perform the flavor separation of the u and d quarks GPDs via linear combinations of proton and neutron GPDs. This paper introduces recent DVCS measurements from the CLAS12 experiment at Jefferson Lab with the upgraded 11 GeV polarized electron beam. Details on the data analysis along with results on Beam Spin Asymmetries are presented.

1 Introduction

Generalized Parton Distributions (GPDs) [1–8] are structure functions that factorize the electroproduction of a photon or a meson on the nucleon. They correspond to the Fourier transform of the QCD non-local and non-diagonal operators and can provide key information in understanding the nucleon structure. The GPDs describe the correlations between the longitudinal momentum and transverse spatial position of the partons inside the nucleon [1, 4, 7, 8], and they give access to the contribution of the orbital momentum of the quarks to the nucleon spin [2, 3]. The nucleon GPDs are accessed in experiments of exclusive lepto-production of a photon (e.g. Deeply Virtual Compton Scattering - DVCS process), or of a meson (e.g. Deeply Virtual Meson Production) off the nucleon at sufficiently large Q^2, where Q^2 is the virtuality of the exchanged photon. This is defined as $-(k - k')^2$, where k and k' are the momenta of the initial and final electrons respectively.

Considering only helicity-conserving quantities and the quark sector, there are four GPDs, $H, \tilde{H}, E, \tilde{E}$, which depend, in leading-order and leading-twist QCD, upon three variables: x, ξ and t (see [1] for more details). The quantities $x - \xi$ and $x + \xi$ are the longitudinal momentum fractions of the quarks coming out and going back into the nucleon, respectively and t is the squared four-momentum transfer between the final and initial nucleon and can equally be defined as $(q - q')^2$, where q and q' are the momenta of the virtual and final real photons respectively. Figure 1 illustrates the leading-order Feynman diagram for DVCS and the definitions of the relevant kinematic variables mainly x_B defined as $x_B = Q^2/2qp$ with p being the initial momentum of the struck nucleon.

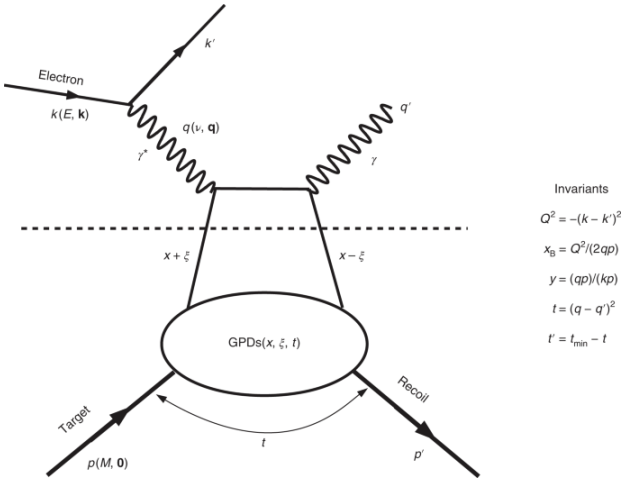

Figure 1. The handbag diagram for DVCS. Kinematical variables are defined in the figure and in the text.

The DVCS process, which naturally interferes with the Bethe-Heitler (BH) process, where the final state photon is emitted by the lepton, allows access to combinations of GPD-related quantities called the Compton Form Factors $CFF(\xi, t)$. In an experimental configuration, where the beam is polarized and the target is unpolarized, one of the accessible observables is the Beam Spin Asymmetry

*e-mail: ajhobart@jlab.org

© The Authors, published by EDP Sciences. This is an open access article distributed under the terms of the Creative Commons Attribution License 4.0 (https://creativecommons.org/licenses/by/4.0/).

(BSA), which relates to the *CFF* as

$$A_{LU} \propto \sin(\Phi)\Im(F_1\mathcal{H}+\xi(F_1+F_2)\mathcal{H}+-kF_2\mathcal{E}+...)\,[9], \quad (1)$$

where Φ is the angle between the lepton scattering and photon production planes, F_1 and F_2 are the Dirac and Pauli form factors, k defined as $k = -t/4M^2$ with M being the nucleon's mass, and $\mathcal{H}$ and $\mathcal{E}$ are the *CFF* related to the GPDs H and E, respectively. The BSA observable will be mainly sensitive to the *CFF* $\mathcal{H}$ of the proton, if the target is a proton, and to the *CFF* $\mathcal{E}$ of the neutron, if the target is a neutron. This is mainly due to the different contributions that arise from the Dirac and Pauli form factors for each nucleon type. Therefore, in order to separate the GPDs of a given nucleon, all the possible experimental configurations need to be considered for the DVCS process with the given nucleon as a target. The quark-flavor separation of the GPDs becomes possible when experimental measurements are performed on both nucleons.

In this paper, we present preliminary results and analysis of the BSA of DVCS from a deuterium target (neutron-DVCS: nDVCS, $ed \rightarrow e'n'\gamma(p)$ and proton-DVCS: pDVCS, $ed \rightarrow e'p'\gamma(n)$; initial electron: e, scattered electron: e', deuterium: d, scattered neutron: n', spectator proton: p, scattered proton: p', spectator neutron: n, photon: γ) using the CLAS12 detector [10] at Jefferson Lab. The GPD E is one of the least known GPDs, and only one previous measurement exists from pioneering experiments performed in Hall-A at Jefferson Lab [11]. However, the experiment reported here is the first measurement with tagging of the active neutron and hence, allowing for a precise determination of the BSA. E is one of the two GPDs that enter into the Ji's sum rule [2, 3], which links the total angular momentum (J_q) carried by each quark q to the sum of the GPDs H and E. The measurement of the GPD H of the bound proton is a first measurement of its kind and is of importance in quantifying nuclear medium effects on GPDs.

2 Experiment and Event Selection

The experiment has taken place in the Hall-B of JLab utilizing the large acceptance spectrometer CLAS12 [10]. The CEBAF accelerator produces a high-intensity, high-duty-factor, polarized electron beam. An average beam polarization of ~85% was measured throughout the experiment in dedicated Møeller scattering measurement runs. The target was an unpolarized liquid deuterium cell measuring 5 cm long. The experiment ran during three different periods, collecting roughly 40×10^9 triggers. A quarter of the data were taken with a 10.6 GeV beam energy, another quarter at 10.2 GeV energy and the other half at 10.4 GeV energy.

To guide the data analysis, in particular for the determination of the process selection, a Monte-Carlo simulation was used. An event generator for incoherent electroproduction of photons on deuterium was adopted, which produces either $ed \rightarrow e'n'\gamma(p)$ or $ed \rightarrow e'p'\gamma(n)$ events, proportionally to their relative cross-sections, coming from the nDVCS/pDVCS and BH reactions [12]. The

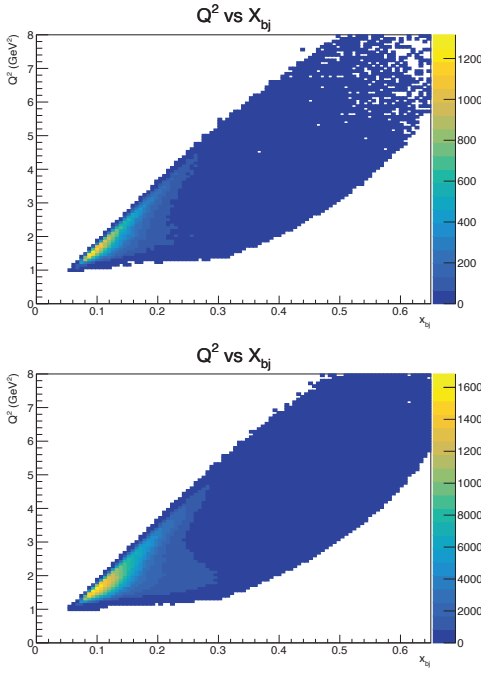

Figure 2. Preliminary. Q^2 versus x_B for the nDVCS data sample (top) and pDVCS data sample (bottom) with all selection cuts applied. The large kinematic reach of CLAS12 is clearly demonstrated in this distribution.

DVCS amplitude is calculated according to the BMK formalism [13]. The Fermi-motion distribution is implemented in the simulations using the Paris potential [14].

Events with at least one identified electron, one photon with energy above 2 GeV, and one nucleon (proton for pDVCS and neutron for nDVCS) with momentum above 0.35 GeV/c were selected. The particle identification of CLAS12 has been used to identify all particles within each event [15]. In the case where multiple final-state particles of the same type are present in the event, all possible combinations of the exclusive final state were considered for treatment. The best combination was taken to be the one minimizing a multi-dimensional χ^2-like quantity calculated using variables related to the exclusive final state.

Several cuts were applied in order to select the relevant kinematic region for the DVCS reactions. The electron momentum was selected to be above 1 GeV/c. We selected nucleon momentum to be above 0.35 GeV/c in order to remove spectator-nucleon events. A cut on the cone angle formed by the electron and the neutron ($\theta_{e,n} < 5°$) was applied to remove radiative photons reconstructed as neutrons. A cut on the cone angle formed by the electron and the photon ($\theta_{e,\gamma} < 5°$) was applied to remove radiative photons that were likely emitted close to the electron. We cut on $Q^2 > 1$ GeV^2/c^2 and $W > 2$ GeV/c to ensure the applicability of the leading-twist GPD formalism and remove contributions from the resonance region. We also require $E_\gamma > 2$ GeV as photons from a DVCS process are expected at high energies. Moreover, fiducial cuts were applied to remove regions where the detector acceptance varies rapidly.

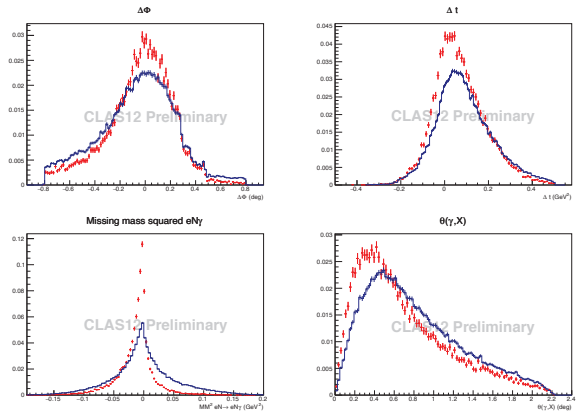

Figure 3. Preliminary. nDVCS data. Top left: $\Delta\Phi$. Top right:Δt. Bottom left: the missing mass in the $en \rightarrow enX$ reaction. Bottom right: the cone angle between the detected and the reconstructed photon $\theta_{\gamma,X}$. Data (in blue) contains background from partially reconstructed π^0 decays. Simulations (in red) of DVCS/BH on deuterium containing both the neutron and proton DVCS/BH channels.

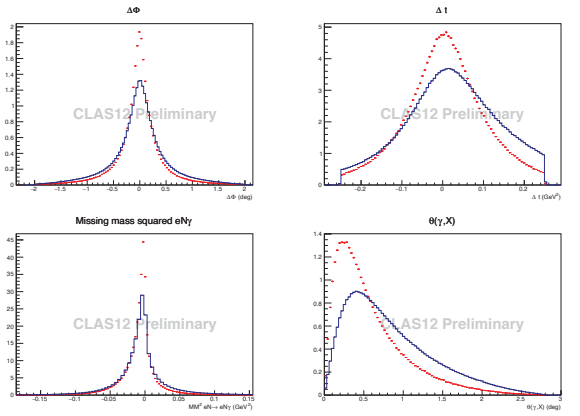

Figure 4. Preliminary. pDVCS data. Top left: $\Delta\Phi$. Top right:Δt. Bottom left: the missing mass in the $en \rightarrow enX$ reaction. Bottom right: the cone angle between the detected and the reconstructed photon $\theta_{\gamma,X}$. Data (in blue) contains background from partially reconstructed π^0 decays. Simulations (in red) of DVCS/BH on deuterium containing both the neutron and proton DVCS/BH channels.

Exclusivity cuts were applied to select the $e'n'\gamma(p)$ and $e'p'\gamma(n)$ final states while minimizing the background. For a nucleon N, cuts on the missing mass in the $ed \rightarrow e'N'\gamma X$, $eN \rightarrow e'N'\gamma X$ and $eN \rightarrow e'N'X$ reactions and the missing momentum in the $ed \rightarrow e'N'\gamma X$ reaction were considered. Cuts were also applied on the difference between the angle Φ between the lepton scattering and photon production planes, computed using the nucleon and the virtual photon and using the virtual and the real photon ($\Delta\Phi$). Similarly, a cut was applied on the difference between two ways to compute t, either using the scattered nucleon or using the virtual and real photon (Δt). Finally, a cut on the cone angle between the detected and the reconstructed photon from the missing particle selection, $\theta_{\gamma,X}$ was applied to reduce the contamination of photons from the partially reconstructed π^0 decay.

Due to inefficiencies in the tracking system of the CLAS12 detector and to the existence of dead regions in the tracker acceptance, some reconstructed neutrons were actually misidentified protons that were cut out using a multivariate analysis technique (Boosted Decision Trees [16]) and utilizing final state exclusivity variables.

Figure 2 shows the two dimensional plane in Q^2 and $x_B = \dfrac{Q^2}{2M\nu}$ after all selection cuts are applied. The distribution clearly shows the large kinematic reach that the large acceptance CLAS12 detector can provide for the measurement of asymmetry observables in the DVCS processes.

Figures 3 and 4 shows some exclusivity variables for the selected $e'n'\gamma$ and $e'p'\gamma$ events in data (in blue) compared to simulations (in red). In order to understand the discrepancies between data and simulations, it is important to know that the data sample contains the background originating from the partially reconstructed π^0 decay produced in the process $ed \rightarrow e'n'\gamma(\gamma(\pi^0), p)$ and $ed \rightarrow e'p'\gamma(\gamma(\pi^0), n)$ where only one of the two photons from the π^0 decay is reconstructed and considered as that of the DVCS process.

The procedure adopted in this analysis to compute the π^0 contamination to the DVCS events sample was done separately for each bin in Q^2, x_B, t and ϕ. The procedure consists of estimating the ratio, in simulations, of partially reconstructed $e'N'\pi^0$(1 photon) decay, selected as if it was true DVCS process, to fully reconstructed, with dedicated exclusive selection, $e'N'\pi^0$ decays. The fact that the ratio is evaluated separately in each bin is beneficial since acceptance and simulation-data discrepancies cancel in the ratio. This ratio, which is obtained from simulations, is expected to be equal to that from data. It is hence applied in data by multiplying it with the number of reconstructed $e'N'\pi^0$ events and therefore evaluating the number of $e'N'\pi^0$(1 photon) in data. The obtained number of $e'N'\pi^0$(1 photon) is subtracted from DVCS reconstructed decays in data for each kinematics bin, and this contamination is evaluated to range between 10-45% depending on the bin under consideration.

3 Extraction of the Beam Spin Asymmetry Observable

The BSA, A_{LU}, is defined as $A_{LU} = \dfrac{1}{P}\dfrac{N^+ - N^-}{N^+ + N^-}$ where P is the average beam polarisation and $N^{+(-)}$ stands for the number of DVCS events for positive (negative) beam helicity. Figures 5 and 6 shows the distribution of A_{LU} for nDVCS and pDVCS respectively, integrated over the measured kinematic domain.

Given the available statistics for nDVCS, we performed an extraction of the BSA in two-dimensional bins in Q^2, x_B or t versus Φ. We considered three bins in Q^2 [1, 1.9], [1.9, 2.9], and [2.9, 6] GeV^2, three bins in X_B [0.05, 0.14], [0.14, 0.2], and [0.2, 0.6] and three bins in $-t$ [0, 0.3], [0.3, 0.5], and [0.5, 1.1] GeV^2. For pDVCS,

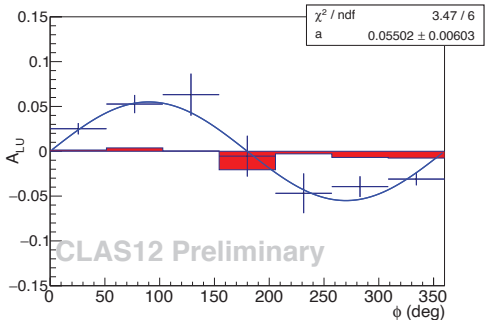

Figure 5. Preliminary. nDVCS BSA integrated over the measured kinematic domain. The distribution is modeled with the function (a sin(Φ)). The red histogram demonstrates the total systematic uncertainty.

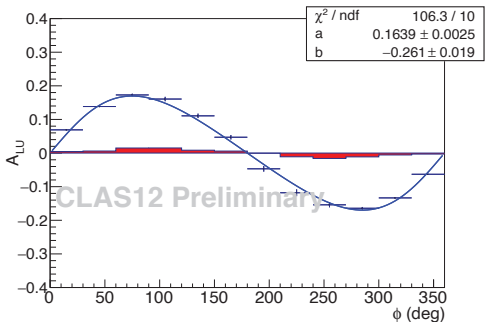

Figure 6. Preliminary. pDVCS BSA integrated over the measured kinematic domain. The distribution is modeled with the function (a sin(Φ)/(1 + b cos(Φ))). The red histogram demonstrates the total systematic uncertainty.

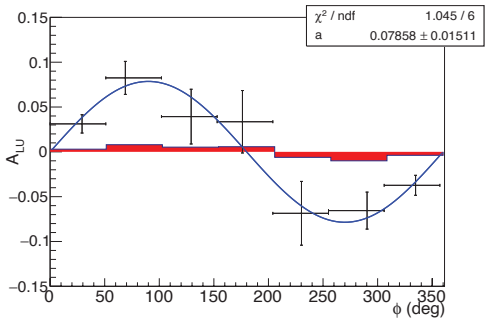

Figure 7. Preliminary. nDVCS BSA of bin in $X_B \in [0.14, 0.2]$. The distribution is modeled with the function (a sin(Φ)). The red histogram demonstrates the total systematic uncertainty.

we performed a 3 dimensional binning of the data in Q^2, x_B and t versus Φ. We considered 5 bins in Q^2 [1,1.6], [1.6,2], [2,2.9], [2.9,3.8] and [3.8,8] GeV^2, 4 bins in X_B [0.04,0.13], [0.13,0.16], [0.16,0.2] and [0.2,0.6] and 3 bins in $-t$ [0, 0.28], [0.28, 0.54], and [0.54, 1.1] GeV^2. Figure 7 shows the BSA of nDVCS in the kinematic bin defined by $X_B \in$[0.14, 0.2] and figure 8 show the BSA of pDVCS in the kinematic bin defined by $X_B \in [0.2, 0.6]$, $Q^2 \in [2.9,3.8]$ GeV^2 and $-t \in [0.54, 1.1]$ GeV^2. The fit function shown in

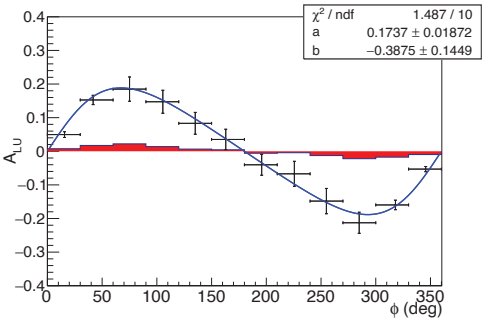

Figure 8. Preliminary. pDVCS BSA of bin in $X_B \in [0.2, 0.6]$, $Q^2 \in [2.9,3.8]$ GeV^2 and $-t \in [0.54, 1.1]$ GeV^2. The distribution is modeled with the function (a sin(Φ)/(1 + b cos(Φ))). The red histogram demonstrates the total systematic uncertainty.

the figures is approximated from physics considerations, however, no physics conclusion is intended from it. A low χ^2 per number of degrees of freedom should not be interpreted as overfitting of the data while a large value might hint to the necessity to include a cos(2ϕ) term in the denominator. Nevertheless, this large χ^2 per number of degrees of freedom is observed on the integrated BSA of pDVCS and can be an effect of integrating over the whole measured kinematic domain. The systematic uncertainties include the uncertainty related to proton contamination cut (for nDVCS BSA only), the uncertainty related to the applied exclusivity selection and the uncertainty on the beam polarization which subsumes the differences between the integrated luminosity for the beam polarization states. The uncertainty related to π^0 subtraction is still under evaluation. Radiative corrections are applied.

4 Conclusions

We have presented the analysis status of nDVCS and pDVCS experimental data obtained from polarized electron beam scattering off a deuterium target. We have observed a positive BSA for nDVCS. The observed BSA for pDVCS is twice as large as that of nDVCS. The integrated BSA of pDVCS is consistent with the integrated BSA observed for a free proton hinting for weak medium effects on the proton GPDs. A more thorough analysis in kinematics bins is to be performed in order to pin any underlying medium effects. The analysis exploits the full kinematic coverage of the CLAS12 detector. Therefore, we performed an extraction of the BSA observable in two-dimensional bins in Q^2, x_B or t versus Φ for the nDVCS BSA and in three-dimensional bins in Q^2, x_B and t versus Φ. Further results, including BSA of DVCS from free proton target can be consulted in [17].

References

[1] D. Müller, D. Robaschik, B. Geyer, F.-M. Dittes, and J. Horejsi. Fortschr. Phys. 42 (1994) 101.
[2] X. Ji, Phys. Rev. Lett. 78 (1997) 610.

[3] X. Ji, Phys. Rev. D 55 (1997) 7114.
[4] A.V. Radyushkin, Phys. Lett. B 380 (1996) 417; Phys. Rev. D 56 (1997) 5524.
[5] J.C. Collins, L. Frankfurt and M. Strikman, Phys. Rev. D 56 (1997) 2982.
[6] K. Goeke, M. V. Polyakov and M. Vanderhaeghen, Prog. Part. Nucl. Phys. 47 (2001) 401.
[7] M. Diehl, Phys. Rept. 388 (2003) 41.
[8] A.V. Belitsky, A.V. Radyushkin, Phys. Rept. 418 (2005) 1.
[9] M. Guidal *et al*. Rep. Prog. Phys. 76 (2013) 066202
[10] V.D.Burkert *et al*., NIM Physics A. 959 (2020) 163419.
[11] M. Benali *et al*., Nature Phys. 16 (2020) 191.
[12] A. El Aloui and E. Voutier, private communication.
[13] A.V. Belitsky, D. Müller, A. Kirchner, Nucl. Phys. B **629** (2002) 323-392.
[14] M. Lacombe *et al*., Phys. Rev C **21** (1980) 861.
[15] V. Ziegler *et al*., NIM Physics A. 959 (2020) 163472.
[16] Y. Coadou, Artificial Intelligence for High Energy Physics, pp. 9-58 (2022) arXiv 2206.09645
[17] G. Christiaens, M. Defurne, D. Sokhan V.Ziegler *et al*., arXiv (2022) 221111274.